JOURNAL OF SPACECRAFT AND ROCKETS
Vol. 46, No. 1, January–February 2009

Thermal Characterization of Emisshield™

Brandon W. Olson*
University of Oklahoma, Norman, Oklahoma 73019
and
Harikishin P. Bakhtiani†
Rocketplane-Kistler Inc., Oklahoma City, Oklahoma 73159

DOI: 10.2514/1.32001

Testing was conducted on a high-emissivity nanoparticle ceramic coating (Emisshield™) for potential use as a high-temperature thermal protection coating on the Rocketplane XP vehicle. Although this product was essentially developed for reentry vehicles, it has broad applicability in other high-speed elevated-temperature applications. This work presents a study of key thermal properties from room temperature up to conditions seen in a mild reentry. Surface-normal emissivity, thermal conductivity, and heat capacity were evaluated as a function of temperature to 760°C (1400°F). Tests were also performed to determine the thermal-cycling durability and potential for reuse of the ceramic coating applied on metal substrates at elevated temperatures.

Nomenclature

C	=	specific heat
k	=	thermal conductivity
Q	=	heat transfer rate
R	=	electrical resistance
T	=	temperature
T_{ss}	=	steady-state temperature
V	=	voltage
$\mathbf{Z}$	=	thermal impedance (complex)
ε	=	emissivity (surface normal)
λ	=	spectral wavelength
ρ	=	density
ω	=	angular frequency

I. Introduction

THE Rocketplane XP belongs to a class of combined naturally aspirated/jet-propelled vehicles designed for use in suborbital applications [1,2]. It is anticipated that these vehicles will be subjected to repeated thermal loading during the mild reentry associated with their proposed mission path. The range of expected operational temperatures for these vehicles exists between those of typical commercial aircraft and fully orbital spacecraft; thus, little surface-coating property data exist in the literature for this midrange region [3–5]. Emisshield™ is a commercial thermal-barrier coating that was originally developed for high-speed reentry of orbital spacecraft but has found use in a wide range of other applications.‡ The objective of this work is to fully characterize the thermal properties of this product over a range of temperatures from room temperature up to 760°C (1400°F), in preparation for its potential use in suborbital reentry applications.

A series of tests were performed at the University of Oklahoma microscale heat transfer lab to determine the thermal characteristics of Emisshield. Experimentally determined properties include surface-normal emissivity, thermal conductivity, specific heat, and thermal-cycling durability of Emisshield.

The surface-normal emissivity of the Emisshield coating was measured using two independent experimental techniques. First, an infrared camera was used to measure the emissivity from 77–288°C (170–550°F). A calibrated thermocouple was used to determine the average sample surface temperature, following which the emissivity setting of the IR camera was adjusted until the measured surface temperature matched that of the thermocouple. The range of measurements with this technique was limited by the effective range of the camera. The second technique used an IR thermocouple and blackbody source to measure the emissivity from 34–760°C (100–1400°F). As before, calibrated thermocouples were used to measure the actual temperature of both the sample and blackbody source. IR measurements of both objects were used in conjunction with a wavelength-dependent formulation of the Stephan–Boltzmann law to determine the effective surface-normal emissivity.

Thermal conductivity of the Emisshield was initially measured using three separate methods: a steady-state method (similar to a guarded hot plate), a sandwiched transient approach, and the 3ω method. Experimentally speaking, in spite of the low thermal conductivity of the Emisshield, its thin coating thickness 0.127 mm (5 mil) lowered its overall thermal resistance to a value that is difficult to measure using standard means. In fact, it was found that surface contact resistance, in both the guarded hot plate and sandwiched transient approaches, introduced an intolerable amount of experimental uncertainty, and thus these results have not been included here. In contrast, the 3ω method uses a thin metallic line element that is placed directly on the material surface and is therefore less sensitive to contact resistance. It is also fundamentally insensitive to parasitic radiative and convective heat loss. The 3ω method thermal-conductivity measurement technique is especially well disposed for measuring the thermal conductivity of films and coatings, and thus it has an inherent advantage for the present application. Although the application of the 3ω method at such high temperatures is atypical, special experimental techniques were developed to overcome problems with thermal expansion and electrical connections. Two substrate materials, aluminum and stainless steel, were tested.

The mass loss and thermal-cycling durability of the Emisshield samples were determined by repeated exposure of the samples to a 538°C (1000°F) environment for durations of 5 min. Sample thicknesses and weight were measured before and after each thermal

Presented as Paper 0417 at the 45th AIAA Aerospace Sciences Meeting and Exhibit, Reno, NV, 7–10 January 2007; received 7 May 2007; revision received 24 May 2008; accepted for publication 2 June 2008.

*Assistant Professor, School of Aerospace and Mechanical Engineering, 865 Asp Avenue, Room 212; bolson@ou.edu.

†Thermodynamics Engineer, 4300 Amelia Earhart Lane. Member AIAA.

‡Data available online at http://www.wessexinc.com/ [retrieved 19 August 2008].

cycle. Both thickness and weight measurements were repeated a number of times to reduce the experimental uncertainty.

II. Test Setup and Procedure

A. Emissivity Measurements

All emissivity measurements are made by referencing some surface of known temperature or emissivity (or both). The first set of emissivity measurements was made using an infrared (IR) camera (FLIR A20). A test jig, equipped with a thermocouple measurement probe (type K), was constructed to hold the sample inside of the testing furnace. Material samples for which the thickness was 0.127 mm (5 mil) (±5%) were provided by the manufacturer on 0.813 mm (0.032 in.) stainless steel 302 substrates. All thermocouples were calibrated over a range from room temperature to 650°C using a dry block calibrator (Ametek CTC 320A). The IR camera was placed at the view port of the furnace, so that the sample was visible in the camera image (see Fig. 1). The temperature of the furnace was allowed to equilibrate, and the sample temperature was measured with the thermocouple probe. The emissivity setting on the camera was adjusted until the average sample surface temperature over a 1 cm^2 area matched (as closely as possible) the thermocouple temperature. Because the camera emissivity is only discretely adjustable, Eq. (1) was used to correct for the remaining temperature mismatch (assuming the camera corrects for ambient environmental temperature):

$$\varepsilon_{\text{measured}} = \varepsilon_{\text{camera}} \frac{T^4_{\text{camera}}}{T^4_{\text{TC}}} \tag{1}$$

The IR camera employed for this experiment had a maximum temperature rating of ~288°C (550°F), and thus it was not possible to employ this technique over the entire test range. A second measurement technique was used that employed an infrared thermocouple (Omega OS37-10K). The IR thermocouple is not equipped with an emissivity setting, and thus it is necessary to have both a reference temperature and a reference surface-emissivity value for comparison. The same calibrated type K thermocouple used in the first experiments was employed again to measure the sample temperature in the furnace. To provide a surface with known emissive properties, a specialized finned test fixture was created to mimic the performance of a black surface (Fig. 1). The special surface treatment and geometric properties of this fixture give it a theoretical emissivity of 0.995. The jig's position within the furnace could be changed during heating to allow either the black surface or the sample surface to be visible within the furnace view port (Fig. 2). When the jig arm containing the sample was aligned with the oven view port, it was positioned to be directly adjacent to the port, thus eliminating any incident radiation originating from the oven interior.

After the furnace had equilibrated, the temperature of the black surface was measured, following which the fixture was shifted sideways to allow the sample temperature to be measured. The standard type K thermocouple measurements were used to calibrate the IR thermocouple by assuming that the black surface has an emissivity of 1. Both calibrated surface temperatures were then used to calculate the surface emissivity using Eq. (2). It should be noted that the IR thermocouple has a finite spectral sensing range (2–20 μm) and that Eq. (2) assumes that the emitted radiation is being measured over the entire EM spectrum. It is possible to correct for this finite sensing range by integrating the emitted spectral energy over the specified sensor range and calculating the emissivity from these corrected values. Calculations show that the amount of correction is less than 1% for all temperature differences in the current study, and thus the full spectrum version is used for simplicity and clarity. Because the IR thermocouple measures the emitted energy with respect to the ambient conditions, this temperature contribution is included in Eq. (2):

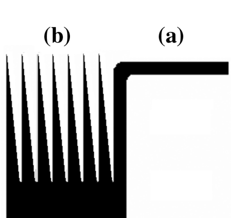

Fig. 1 Design of blackbody test jig: the sample is mounted on the jig arm (a), and the finned portion (b) closely approximates a black surface. The jig is constructed of copper and coated with high-emissivity high-temperature paint.

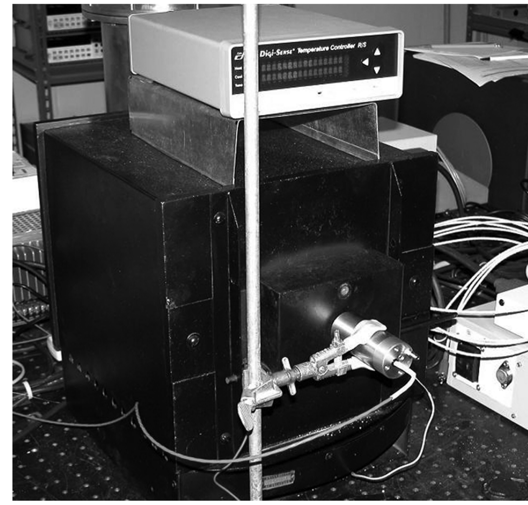

Fig. 2 Emissivity measurement using an IR thermocouple. The sensor is positioned at the furnace view port to provide an unobstructed view of the sample.

$$\varepsilon_{\text{measured}} = \frac{T^4_{\text{IR}_{\text{TC}}} - T^4_{\infty}}{T^4_{\text{BB}} - T^4_{\infty}} \tag{2}$$

The results of Eq. (2) will be a spectrally averaged emissivity value or the emissivity value associated with the total surface heat transfer. The manufacturer of Emisshield asserts that the coating is a true gray surface for which the properties are not spectrally dependent. Although these measurements were not made using wavelength-sensitive equipment, this feature can be generally observed by the fact that the emissivity does not display strong temperature dependence. Generally, as the surface temperature changes, the emission spectrum will shift and any change in spectral properties will manifest itself as a change in the total or average emissivity.

B. Thermal Conductivity Measurements

The 3ω method is a frequency-based technique for measuring thermal properties that employs a wire element as both a heat source and temperature measurement device [6,7]. Typically, wire test elements are patterned on the surface of the sample using photolithography, as illustrated in Fig. 3, yet for irregularly shaped or porous samples, this fabrication technique does not work. The author has developed an alternative approach that bonds a commercially drawn wire test element, for which the diameter is typically between 5 and 25 μm, to the surface of the sample material [8]. Figure 4 illustrates how these wire elements are placed on the material surface and electrically connected to external instruments. Because the sensing wire is mounted directly to the surface, the 3ω method is especially well disposed for measuring the thermal conductivity of films and coatings, and thus it has an inherent advantage for the present application.

Use of 3ω at such high temperatures is atypical, principally because of the difficulties associated with thermal expansion of the sample and the wide-ranging variation in sample resistance. The samples were tested in an atmospheric-pressure high-temperature furnace. The bridge cancellation circuit used in 3ω testing [8] was modified to include a wide-range potentiometer that could accommodate the large thermally induced changes in sample

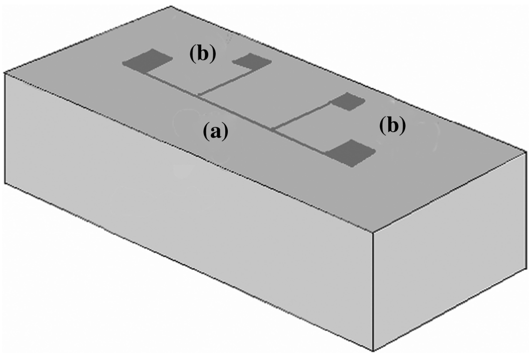

Fig. 3 Schematic image of a 3ω element: the 3ω wire (a) is connected in a 4-wire configuration with voltage and current connections at (b).

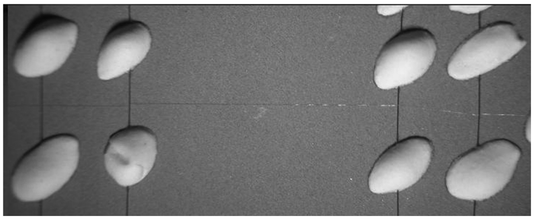

Fig. 4 Commercial wire 3w element: the test wire is positioned on the surface of an Emisshield sample. White dots are high-temperature epoxy designed to keep the voltage lead wires (vertical wires on the left and right) from moving. The horizontal test wire is held in place by a thin (∼10 μm) spin-on glass layer.

electrical resistance. During initial experiments, the wire elements delaminated at temperatures between 350 and 400°C. In an effort to solve this problem, the wire-element material was changed to nickel, for which the thermal-expansion coefficient more closely matched that of the most common substrate material (stainless steel).

Experimental measurements were made using a specialized LabVIEW-based data acquisition and control program. This program controls the temperature spacing of each measurement, bridge balancing, and frequency and voltage settings. At each measurement temperature, the sample was allowed to equilibrate for approximately 30 min, or until the temporal variation was less than 0.1°C. The electrical circuit bridge was balanced to eliminate unwanted signal components, and the third harmonic voltage was measured at each frequency point (typically 20). Each frequency scan required approximately 1 min to execute. All temperature and voltage measurements were recorded to a data file. Each experimental run required approximately 6–7 h to complete.

The 3ω method measures thermal properties by scanning a range of voltage frequencies and then measuring the thermal response at each frequency. Experimental measurements were reduced to material properties using a specially developed least-squares algorithm (coded in MATLAB® script language) based on an unapproximated analytical model [8]. Traditionally, 3ω was only used to measure thermal conductivity of bulk materials; however, this specialized program can also be used to determine the sample thermal conductivity of homogenous and multilayer samples [9].

The analytical model that was used as a basis for the least-squares algorithm was formulated in terms of impedance, or frequency thermal resistance. The impedance can be mathematically defined as

$$\mathbf{Z} = \frac{\mathbf{T}}{\mathbf{Q}} \tag{3}$$

In Eq. (3), **Z** represents the thermal impedance and **T** and **Q** are the periodic surface temperature and heat transfer rate, respectively. Bold quantities indicate a complex value that consists of both in-phase and out-of-phase components. Example impedance values for an Emisshield sample from the current study are plotted in Fig. 5.

An impedance formulation lends a greater physical interpretation to experimental measurements by permitting direct comparison of results between temperatures and even between samples. Low-conductivity materials display correspondingly higher thermal impedance (larger amplitude), whereas materials with a high heat capacity exhibit larger amounts of phase lag (the out-of-phase component is proportionately larger). Also, the impedance is seen to decrease at higher frequencies, where the thermal penetration depth is smaller. Thus, using an impedance plot, it is possible to qualitatively determine how thermal conductivity and heat capacity are changing at different temperatures and for different samples.

One obvious concern for thermal-conductivity measurement is parasitic heat loss through the competing modes of convection and radiation. The effect of radiation heat loss on the 3ω method can be estimated using an expansion of the general equation for radiation heat flux [10]:

$$Q_{\mathrm{rad}} = \sigma \varepsilon A \left(T^4 - T_{\mathrm{ss}}^4\right) \tag{4}$$

The 3ω element is resistively heated by a voltage at a frequency of ω, which produces Joule heating at a frequency of 2ω. The wire temperature can be represented by combining steady-state and transient components:

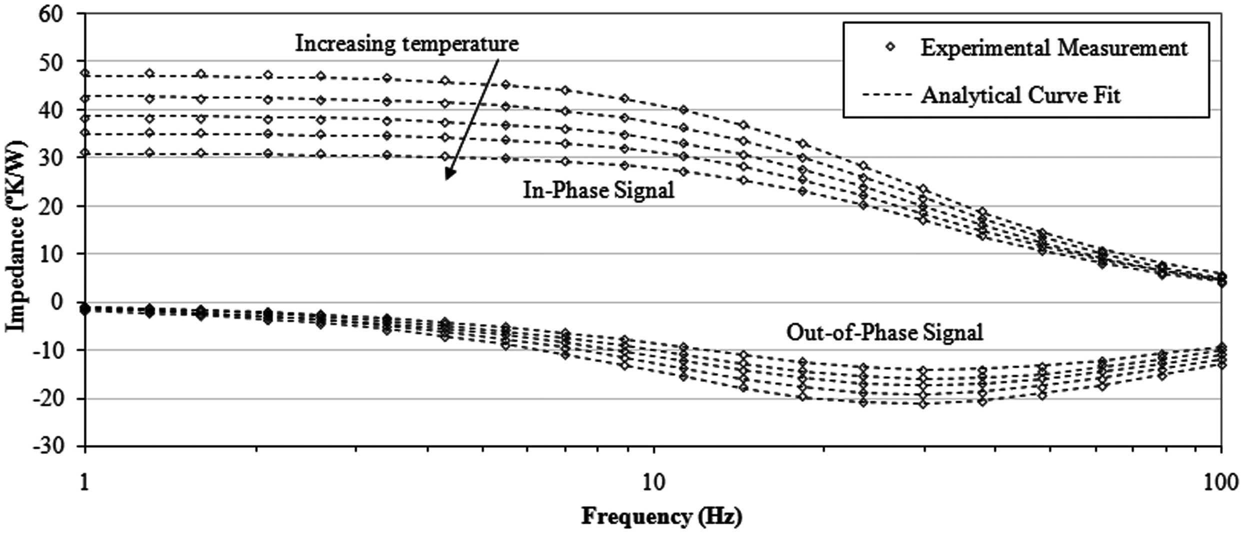

Fig. 5 Impedance values for 3ω experimental measurements are plotted versus driving frequency. Results from the analytical model curve fit are also shown.

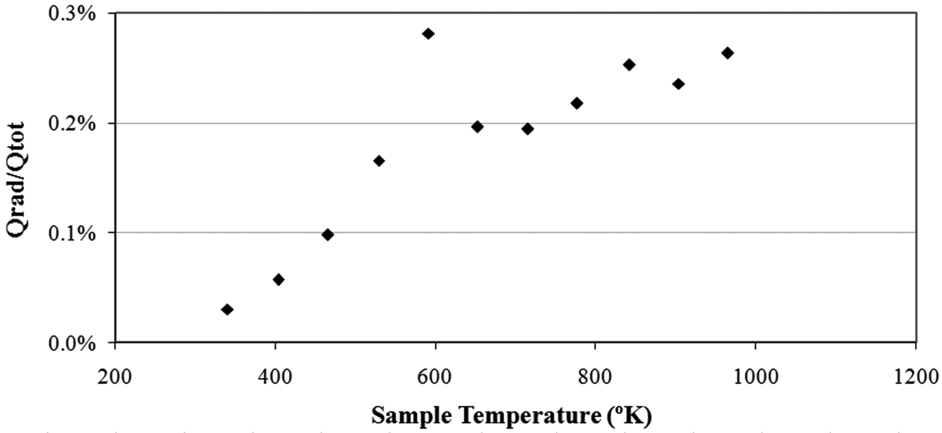

Fig. 6 Effect of radiation losses on 3ω measurements. The experimental measurements taken from a nickel wire/stainless steel substrate Emisshield sample were used to estimate the ratio of radiative losses to the total electrical power input. Although the effect of the parasitic losses increases with temperature as expected, its total magnitude is still less than 1% and is therefore totally negligible.

$$T = T_{ss} + \Delta T \cos(2\omega) \tag{5}$$

Equation (5) can be used to estimate the T^4 term that appears in Eq. (4):

$$T^4 = T_{ss}^4 + 4T_{ss}^3 \Delta T \cos(2\omega) + 6T_{ss}^2 \Delta T^2 \cos^2(2\omega) + 4T_{ss} \Delta T^3 \cos^3(2\omega) + \Delta T^4 \cos^4(2\omega) \tag{6}$$

The contributions of the higher-order cosine terms will be minimal because $T_{ss} \gg \Delta T$, and they will principally occur at frequencies other than 2ω and thus they can be neglected. The remaining terms can be written as follows:

$$Q_{rad} = \sigma \varepsilon A (4T_{ss}^3 \Delta T) \tag{7}$$

The radiation heat loss can be compared with the total electrical power being dissipated in the element to give a rendering of its magnitude:

$$\frac{|Q_{rad}|}{|Q|} = \frac{4\sigma \varepsilon A T_{ss}^3 \Delta T}{V^2/2R} \tag{8}$$

Experimental parameters from an Emisshield sample in the current study were used in conjunction with Eq. (8) to estimate the parasitic radiative losses. Figure 6 shows that under the current operating conditions, the radiative losses are completely negligible. A similar analysis for convective transfer demonstrates even smaller losses.

C. Mass Loss and Coating Durability Measurements

Emisshield samples on both types of substrates (aluminum and stainless steel) were subjected to two sets of temperature cycling in a furnace preheated to 538°C (1000°F). Each of the two cycles consisted of 5 subcycles in which the substrates were placed in the equilibrated furnace for 5 min and allowed to cool at room temperature for 5 min. These tests were designed to detect mass loss, appreciable changes in dimension, and any surface irregularities that may occur during high-temperature thermal cycling. Thickness dimensions, weight, and surface images were recorded for each of the samples before and after temperature cycling. Thickness measurements for each set were taken at 9 different locations on the samples and averaged.

III. Experimental Results

A. Emissivity Measurements

Surface-normal emissivity measurements for two Emisshield samples are plotted in Fig. 7. Both of these test samples had stainless steel as a substrate material because the aluminum substrates were not capable of withstanding the higher portion of the temperature range (due to material softening). Measurements taken with the IR camera and IR thermocouple display good agreement in the overlapping region and fall within the range of values listed by the manufacturer (Wessex, Inc.) for a family of products in this class of protective ceramic coatings (PCC). Although it is not exactly identical, manufacturer's data were provided for a similar formulation of PCC and are plotted here for comparison.

B. Thermal Conductivity and Heat Capacity Measurements

The measured thermal-conductivity values for several Emisshield samples are plotted in Fig. 8. The thermal conductivity of Emisshield lies within the conductivity range associated with glassy or ceramic materials and is hence an excellent choice for thermal-barrier applications. The thermal conductivity does, however, display a general upward trend that is not typical of most insulative materials.

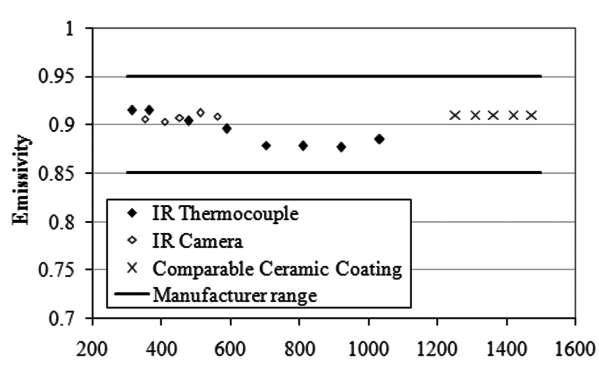

IR-TC		IR-Camera	
T (°K)	ε	T (°K)	ε
273	0.915	354	0.906
273	0.915	409	0.903
273	0.904	454	0.908
273	0.896	514	0.912
273	0.879	562	0.908
273	0.878		
273	0.877		
273	0.885		

Fig. 7 Surface-normal emissivity of Emisshield. Emisshield thickness for these experiments was 0.127 mm (5 mil) and the substrate material was stainless steel. Measurements from both the IR camera and IR thermocouple are included, along with manufacturer's data for similar PCC.

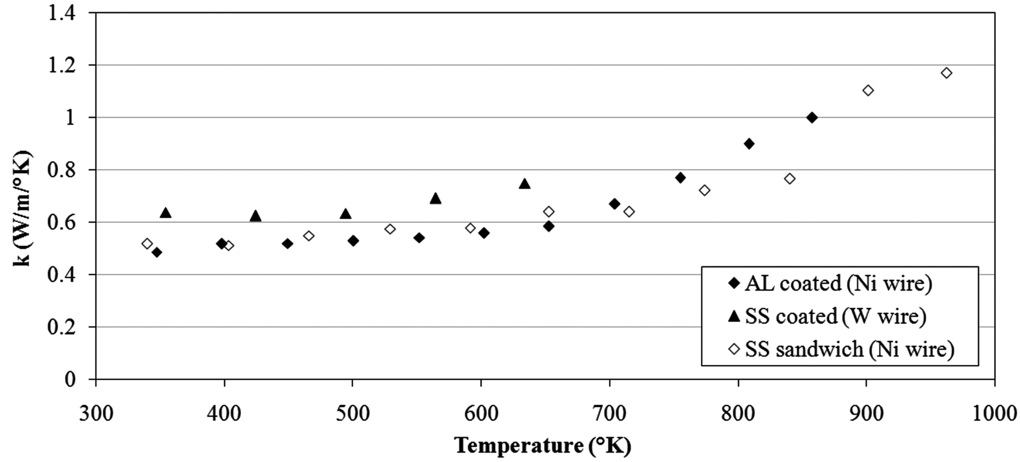

Fig. 8 Emisshield thermal-conductivity values measured using 3ω. All coatings were 0.127 mm (5 mil) in thickness. Both aluminum and stainless substrates were tested with surface-mounted (coated) and sandwiched test wires.

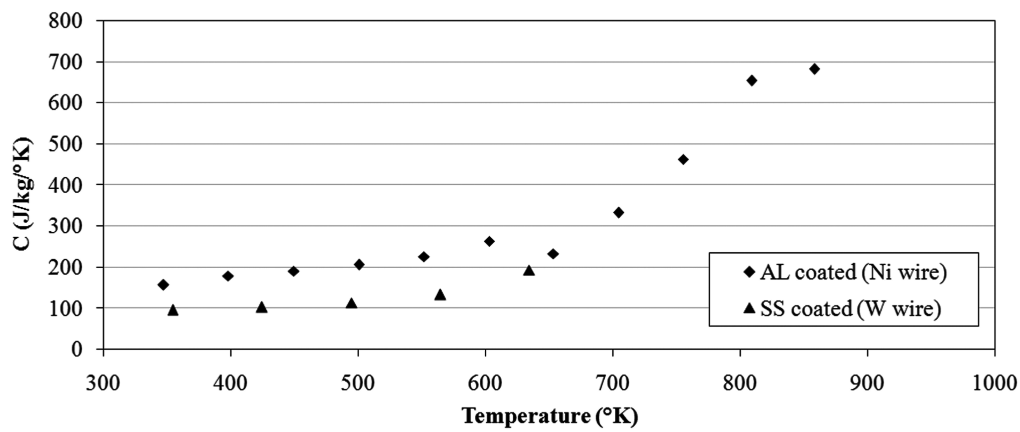

Fig. 9 Emisshield specific-heat values measured using 3ω. Samples tested using the sandwich method exhibited large contact resistance that introduced an unacceptable amount of uncertainty in the heat capacity measurements and are not listed here.

This behavior does, however, correspond well to other thermal-barrier coatings in the literature in both magnitude and trend [11]. It has been speculated that this increase in heat transfer may be due to improved radiative heat transfer *within* the porous material structure. However, based on order-of-magnitude estimations, it appears that internal radiation heat transfer would most likely not play a significant role at the temperatures used during testing. Given that the samples display no appreciable change in properties even after significant heating, it can be assumed that there was no morphological change in material properties as a result of high-temperature treatment.

The measured specific-heat values for several Emisshield samples are plotted in Fig. 9. The measured values fall within the range that could be expected of highly porous ceramic materials. It should be noted that the 3ω method actually measures heat capacity ρC. The value of the specific heat was determined using an independent measurement of the density of the Emisshield by weighing and measuring a substrate with and without the coating.

C. Mass Loss and Coating Durability

The weight-change measurements for the Emisshield samples during each of the two temperature cycles are tabulated in Table 1, which reports the average weight change during the first and second temperature cycles as well as the estimated percent of weight change of the coating. A measurable change in weight was observed on both samples during the first cycling. There appeared to be no appreciable change in weight in the second cycling

Following the first cycling, all three samples displayed a measurable decrease in weight: ~0.049 g on average (~2% by weight). There was no substantial change in sample weight following the second cycling. The thickness measurements that were recorded before and after the temperature cycling showed no apparent change for either trial. It can be theorized that the initial weight change is either due to unevaporated solvents in the Emisshield coating or atmospheric moisture that had been absorbed during shipping and handling. Several of the substrates were observed to warp slightly during testing, but the Emisshield coating was not observed to delaminate or sustain any visible damage during the thermal cycling.

IV. Conclusions

The present work has illustrated that the two key performance parameters of Emisshield, the emissivity and thermal conductivity, both tend to degrade slightly at elevated temperatures (below 1000 K). The emissivity tends to decrease from 0.915 to 0.876 (~4%) over the range from room temperature up to 1000 K. The thermal conductivity tends to roughly double from 0.6 to

Table 1 Mass loss measurements for Emisshield

Temp. cycle	AI	SS
Weight change, g		
1	−0.052	−0.045
2	0.004	0.002
Estimated Emisshield weight change, %		
1	−2.3%	−1.7%
2	0.2%	0.1%

1.2 W/m/K over the same temperature range. Although both parameters degrade somewhat, it is not likely that these changes would preclude their use in a mild reentry application or in most other commercial applications. Indeed, given the effective operational range of this coating and its excellent thermal properties and apparent durability, it would likely outperform most comparable coatings.

References

[1] Raymer, D. P., and Clapp, M. B., "Pioneer Rocketplane Conceptual Design Study," *Journal of Aircraft*, Vol. 39, No. 3, 2002, pp. 507–511.

[2] Brauckmann, G. J., "X-34 Vehicle Aerodynamic Characteristics," *Journal of Spacecraft and Rockets*, Vol. 36, No. 2, 1999, pp. 229–239.

[3] Levy, D. W., Wariner, D. L., and Nelson, R. E., "Validation of Computational Euler Solutions for a High Speed Business Jet," 12th Applied Aerodynamics Conference, Colorado Springs, CO, AIAA Paper 94-1843, June 1994.

[4] Engel, C. D., "Orbital Entry Aerodynamic Heating Evaluator," Qualis Corp., TR [01050]-TR-2002-13, Huntsville, AL, Sept. 2002.

[5] Raymer, D. P., *Aircraft Design: A Conceptual Approach*, 3rd ed., AIAA Education Series, AIAA, Reston, VA, Sept. 1999.

[6] Cahill, D. G., "Thermal Conductivity Measurement from 30 to 750 K: The 3ω Method," *Review of Scientific Instruments*, Vol. 61, No. 2, 1990, p. 802.
doi:10.1063/1.1141498

[7] Olson, B. W., Graham, S., and Chen, K., "A Practical Extension of the 3ω Method to Multilayer Structures," *Review of Scientific Instruments*, Vol. 76, No. 5, 2005, Paper 053901.
doi:10.1063/1.1896619

[8] Olson, B., and Garikapati, C., "Extending the 3ω Method: Experimental Simplification and Analytical Improvements," *Thermal Analysis and Calorimetry* (to be published).

[9] Olson, B., and Graham, S., "Extending the 3 Omega Method to Measure Thermal Conductivity Anisotropy in Three Dimensions," *Proceedings of the ASME Summer Heat Transfer Conference*, Vol. 1, American Society of Mechanical Engineers, New York, 2005, p. 29.

[10] Siegel, R., and Howell, J. R., *Thermal Radiation Heat Transfer*, 3rd ed., Taylor and Francis, Philadelphia, 1992, Chaps. 7, 8.

[11] Zhu, D., and Miller, R. A., "Thermal Conductivity and Elastic Modulus Evolution of Thermal Barrier Coatings Under High Heat Flux Conditions," NASA/TM Paper 1999-209069, 1999.

G. Palmer
Associate Editor